Nonlinear Coastal and Equatorial Jets

S. G. H. PHILANDER

Geophysical Fluid Dynamics Laboratory/NOAA, Princeton University, Princeton, NJ 08540

(Manuscript received 27 November 1978, in final form 19 February 1979)

ABSTRACT

Nonlinearities weaken westward equatorial jets and cause them to be shallower and broader than their linear counterparts. Nonlinear eastward equatorial jets, on the other hand, are more intense, deeper and narrower than linear jets. Since nonlinear effects are important on time scales longer than about one week, winds that fluctuate on such time scales introduce hysteresis effects and can generate flow with a complicated vertical structure in the surface layers of the equatorial oceans. Coastal jets differ from equatorial jets in that they are only weakly influenced by nonlinearities; this result could change if alongshore pressure forces are taken into account.

1. Introduction

Winds parallel to the equator or a coast readily generate intense equatorial or coastal jets. This happens, for example, in the Indian Ocean when the eastward winds along the equator intensify suddenly (Wyrtki, 1973; Knox, 1976). For a description of coastal jets see Mooers *et al.* (1976). These various jets accelerate constantly once they are in geostrophic balance so that they are bound to become nonlinear. This paper concerns the effect of nonlinearities on the structure of coastal and equatorial jets. To study the nonlinear problem we use a two-dimensional numerical model; variations in a direction parallel to the coast or equator are neglected. The model ocean has a realistic stratification which is chosen such that the equivalent depths of the first few baroclinic modes are also realistic. The flat floor of the ocean is at a depth of 3000 m and the coasts are vertical. This is unrealistic as far as coastal regions are concerned, but it permits an investigation of nonlinear effects on a time scale short compared to that on which dissipation is dominant. [Allen (1973) shows that a dissipative steady state is approached on a time scale that depends on the vertical Ekman number.] The model to be used here is described in detail in Section 2. Sections 3 and 4 concern zonal equatorial jets generated by zonal and meridional winds respectively. Section 5 describes coastal jets and Section 6 is a discussion of the results.

2. The model

Let x, y, z be the eastward, northward (from the equator) and upward (from the ocean surface) coordinates. (Alternatively, let x and y denote coordinates parallel to and perpendicular to the coast, respectively.) Let u, v, w be the corresponding velocity components. We assume that the flow is independent of x so that a streamfunction can be introduced:

$$v = \psi_z, \quad w = -\psi_y. \tag{1}$$

If we make the hydrostatic approximation, the vorticity for motion in the y-z plane is

$$\zeta = \psi_{zz}. \tag{2}$$

The equations of motion for a Boussinesq fluid can now be written

$$\zeta_t - J(\psi,\zeta) + fu_z = \frac{g}{\rho_0}\rho_y + \nabla\cdot(\nu\nabla\zeta), \tag{3a}$$

$$u_t - J(\psi,u) - f\psi_z = \nabla\cdot(\nu\nabla u), \tag{3b}$$

$$\rho_t - J(\psi,\rho) = \nabla\cdot(K\nabla\rho). \tag{3c}$$

Here f is the Coriolis parameter, which is a constant for coastal problems and equal to βy for equatorial problems, g is the gravitational acceleration, t measures time, J denotes a Jacobian, ν and K represent coefficients of eddy diffusion and ρ is the density.

The appropriate boundary conditions are

$$\nu u_z = \tau^x, \quad \nu\zeta = \tau^y, \quad \psi = 0, \quad \rho_z = 0$$

at

$$z = 0, \tag{4a}$$

$$u = 0, \quad \zeta = 0, \quad \psi = 0, \quad \rho_z = 0$$

at

$$z = -H. \tag{4b}$$

At vertical boundaries that bound the domain we impose the conditions

0022-3670/79/040739-09$06.25

$$\psi = u_y = \rho_y = \zeta = 0. \quad (4c)$$

These equations are solved numerically by using a computer program developed by Orlanski and Ross (1973) and Orlanski *et al.* (1974). A centered space and time difference approximation is used to represent the space and time derivatives. The Jacobians are treated by the methods of Arakawa (1966) and Lilly (1965) to minimize nonlinear instability. The leapfrog method is used for time differencing but with the diffusive terms lagged one time step. The solution is time-smoothed every 30 time steps to minimize mode splitting.

The depth of the ocean is taken to be 3000 m and the 61 levels in the vertical are spaced nonuniformly (see Fig. 1). Initially the ocean is motionless and the density field ρ is a function of depth only. It is assumed that

$$\rho = \rho_0(1 - \alpha T),$$

where $\alpha = 0.0002°C^{-1}$. Fig. 1 shows the initial temperature field and the associated Brunt-Väisälä frequency N. [Below a depth of 500 m, N has a constant value and the temperature T decreases linearly, to zero in case a (Fig. 1a) and to 5°C in case b (Fig. 1b).] For the equatorial ocean the equivalent depths and associated radii of deformation for the first few baroclinic modes are (71 cm, 365 km), (27 cm, 286 km) and (14.5 cm, 245 km). For the coastal ocean the corresponding scales are (50 cm, 22 km), (16 cm, 12.5 km) and (9 cm, 9.5 km) at 45°N.

The equatorial ocean is bounded by walls 1500 km from the equator and has a latitudinal resolution of 30 km. The coastal ocean is bounded by a wall 300 km from the coast of interest, and has a resolution of 6 km. Errors due to finite differencing are minimized by using a staggered grid.

The coefficient of vertical eddy viscosity ν_v has a value equal to 20 $cm^2\ s^{-1}$ at the first 5 grid points (i.e., in a 35 m deep mixed layer) and has a value equal to 1 $cm^2\ s^{-1}$ at greater depths. The coefficient of horizontal eddy viscosity ν_H has a value equal to 1000 ν_v. We assume that $K_v = \nu_v$ and $K_H = \nu_H$. In some experiments (not described here) we assumed $\nu_v = 20\ cm^2\ s^{-1}$ everywhere or we assumed a more complicated function of depth for ν_v but such changes appeared to have little effect on the results for the first three weeks of integration.

Because the fluid is diffusive, the initial temperature field changes even in the absence of any forcing. (Temperatures decrease uniformly above the thermocline and increase uniformly below the thermocline.) Calculations for different values of K_v show that the velocity field and the latitudinal structure of the density field are relatively insensitive to K_v.

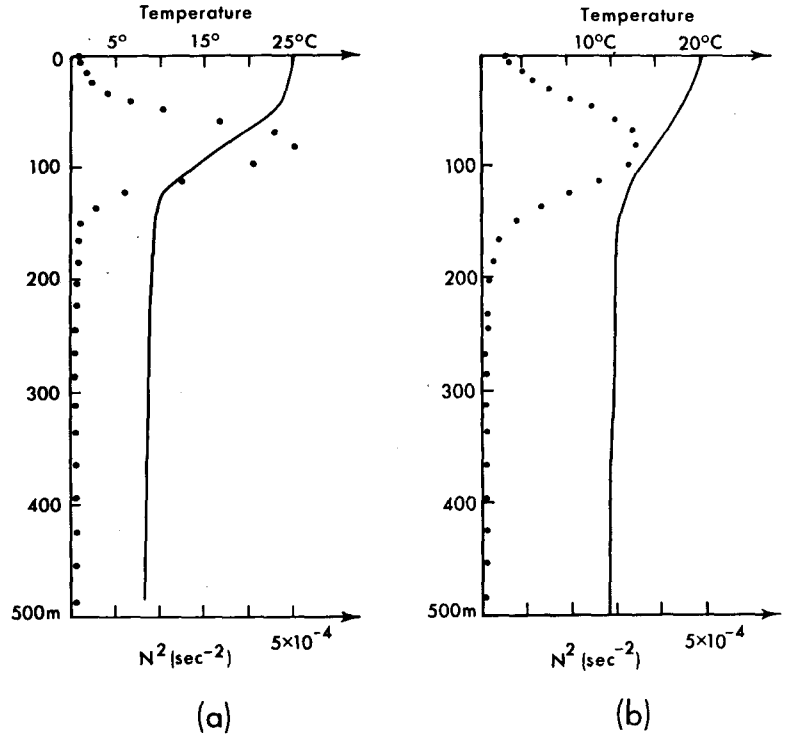

FIG. 1. The initial temperature and initial Brunt-Väisälä frequency, in the upper 500 m of the model equatorial (a) and coastal (b) ocean. The black dots show the grid points.

3. The response of an equatorial ocean to zonal winds

In an ocean initially at rest, winds parallel to the equator generate an intense equatorial jet, but only after a certain time has elapsed, because there is nothing distinguishing about the equator while the effects of rotation are secondary. Fig. 2 clearly shows that 1.5 days after the sudden onset of the winds, the scale of the motion is simply determined by the distance between the boundaries of the domain. (The equator acts as a wall because it is a line of symmetry.) By day 4.5 an equatorial jet has developed and after a week the displacement of the isotherms indicate that the jet is in geostrophic balance. Fig. 3 shows the evolution of the latitudinal structure of the jet. Note that the half-width of the distinctly equatorial jet is 250 km. Which parameters determine these time and space scales?

In a constant-density ocean of depth h the jet is in geostrophic balance after an adjustment period equal to $1/(\beta^2 gh)^{1/4}$, by which time it has a half-width equal to $(gh/\beta^2)^{1/4}$ (Yoshida, 1959; O'Brien and Hurlburt, 1974; Moore and Philander, 1977). These results are thought to be relevant to baroclinic motion in the ocean provided the depth h is the equivalent depth of a dominant baroclinic mode.

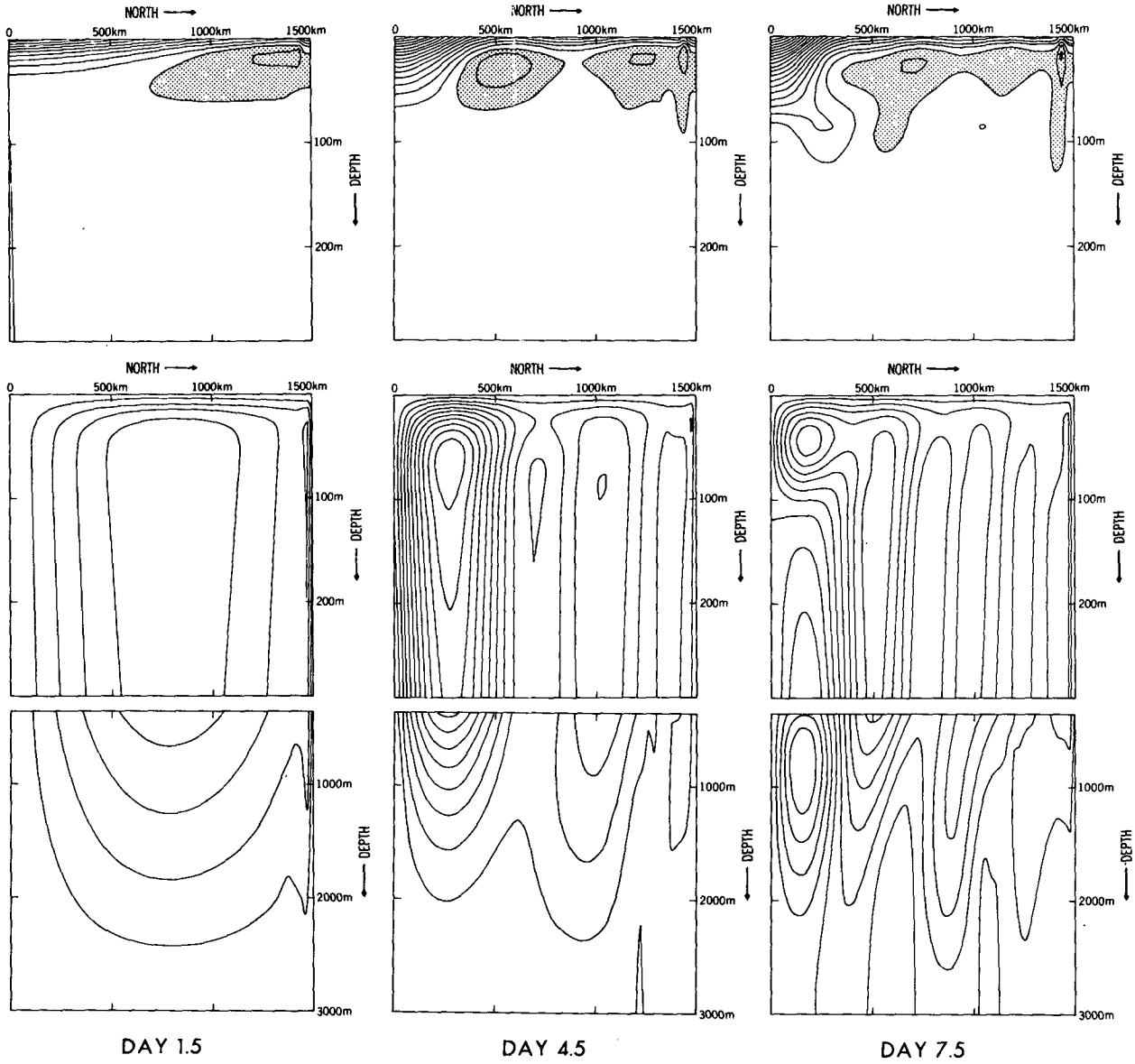

FIG. 2. The zonal velocity (upper row of plates) and streamfunction (two lower rows of plates) 1.5, 4.5 and 7.5 days after the sudden onset of winds of intensity 1 dyn cm^{-2} over a linear equatorial ocean. Contours are at intervals of 10 cm s^{-1} and 10^3 m^2 s^{-1}, respectively.

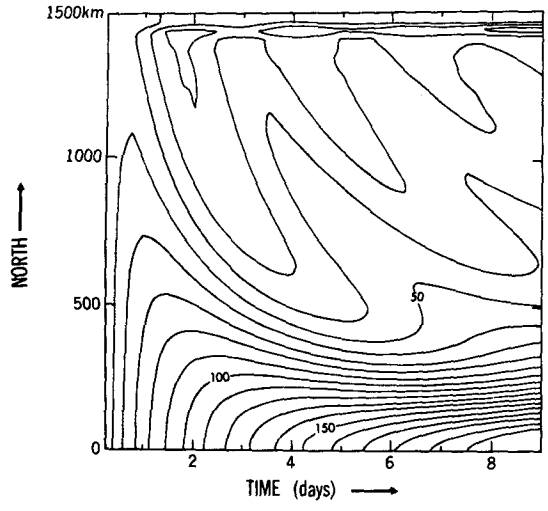

FIG. 3. The evolution of the latitudinal structure of the equatorial jet at the surface.

The first baroclinic mode usually is assumed to be dominant. It is evident from Fig. 2 and the middle panel of Fig. 4 that the vertical structure of the jet does not coincide with that of any single vertical mode. It therefore seems that the above expressions for the adjustment time and half-width are inappropriate. Consider, furthermore, an infinitely deep ocean with constant Brunt-Väisälä frequency N. In this ocean vertically standing modes are impossible, and a discrete set of equivalent depths are not available. However, zonal winds will still generate an equatorial jet. What determines its spatial and temporal scales in this case?

The main problem is to decide what the vertical scale of the motion is because once such a scale is known, a horizontal scale, namely, the radius of deformation, can immediately be calculated.

We consider the linear, longitude-independent response of the ocean to a zonal wind stress τ^x which acts as a body force in a surface layer of depth D. Since the flow is symmetrical about the equator the zonal momentum equation at the equator is

$$u_t = \tau^x/D. \tag{5}$$

(The ocean is assumed to be nondiffusive; t denotes time.) At the equator there is zonal motion only in the surface layer of depth D where the flow accelerates uniformly. Should this ocean have a discrete (and complete) set of vertical modes then the relatively simple vertical structure of the flow at the equator, as inferred from (5), can be described in terms of these modes. But it is not clear (for arbitrary stratification) that any one of these modes is dominant, and that its equivalent depth is the appropriate vertical scale from which to calculate the width of the current. Instead, the depth D is a much more obvious vertical scale. The equatorial radius of deformation for constant stratification N is then $(ND/\beta)^{1/2}$ (which is the scale of the half-width of the jet), and the appropriate temporal scale is $(ND\beta)^{-1/2}$.

Instead of having the flow driven by a body force in a layer of depth D, one can assume a wind stress on a diffusive ocean so that (5) is replaced by

$$u_t = \nu u_{zz}. \tag{6}$$

[The middle panel of Fig. 4 is essentially the solution to Eq. (6)]. Moore (1979) has studied the linear response of such a diffusive, infinitely deep ocean, with constant stratification N, to the sudden onset of zonal winds. Just outside the equatorial zone there is an Ekman layer of depth $h_E = \sqrt{\nu/f}$ and below that is a stratified layer of depth $h_s = fL/N$, where L is a horizontal length scale imposed by the Ekman suction. At the equator momentum diffuses downward according to (6) so that the depth scale there depends on the coefficient ν. Once this depth scale is determined from a scale analysis, it replaces D in our earlier expression for the equatorial radius of deformation. This is the half-width of the

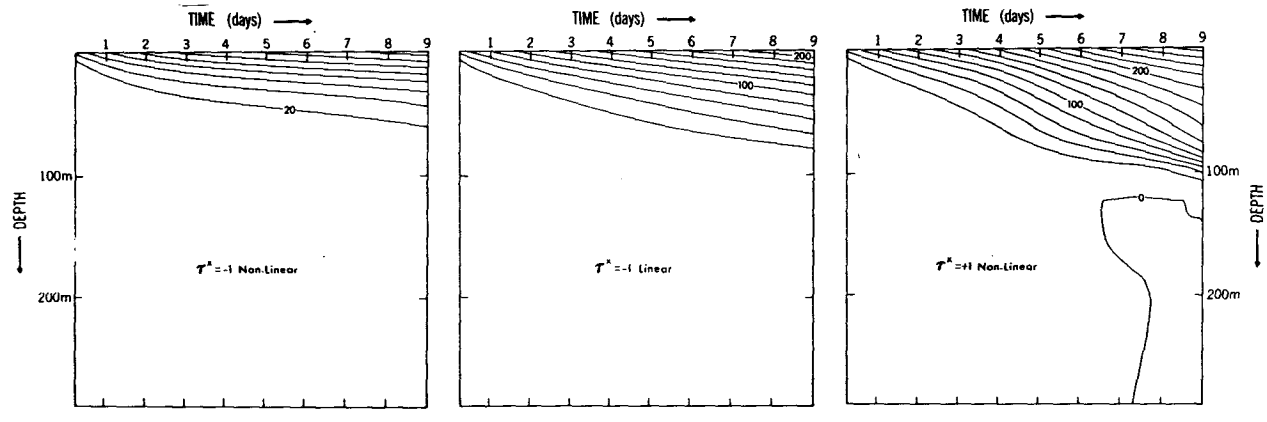

FIG. 4. The zonal velocity component at the equator as a function of time and depth. Contours are at intervals of 20 cm s^{-1}. Flow is in the wind direction.

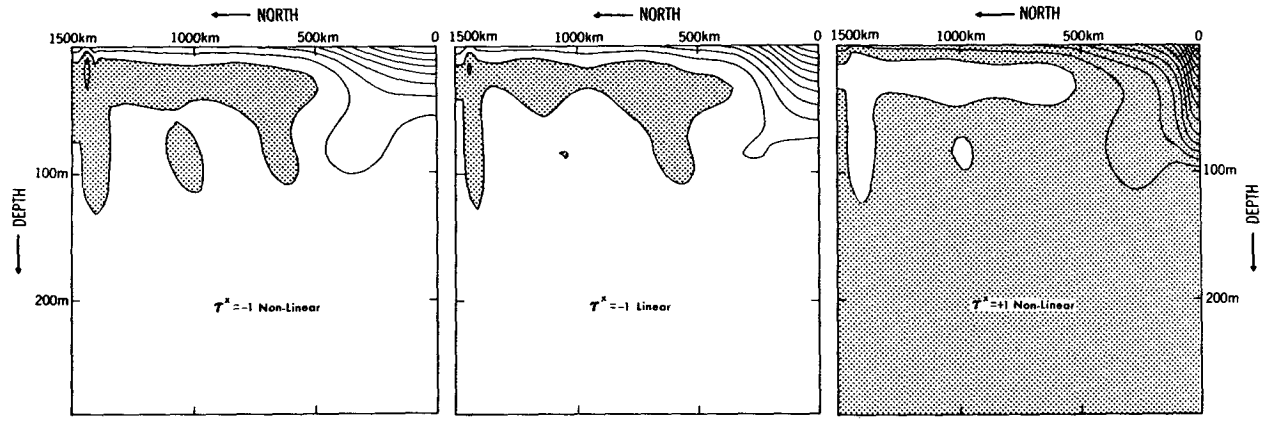

FIG. 5. The zonal velocity component, as a function of latitude and depth, 7.5 days after the sudden onset of zonal winds of intensity 1 dyn cm^{-2}. Contours are at intervals at 20 cm s^{-1}; regions of eastward flow are shaded.

accelerating equatorial jet in Moore's solution. The main point is that the wind-generated jet is a surface phenomenon and is not affected by the stratification of the deep ocean. It is therefore inappropriate to use as a depth scale the equivalent depth of a vertically standing mode whose structure depends on the stratification of the entire water column.

For the jet in our model the appropriate length scale is the radius of deformation $(N_0D/\beta)^{1/2}$, where from Fig. 1, D = 100 m is the depth of the thermocline and $N_0 = 2.10^{-2}$ s^{-1} is a representative value of N in the thermocline. This gives a numerical value for the half-width of the jet of about 250 km. (The radius of deformation associated with the first baroclinic mode is 365 km.) The adjustment time $(N_0D\beta)^{-1/2}$ is about a week.

According to linear theory, the flow at the equator is governed by the diffusion equation (6) so that vertical diffusion will ultimately be important at all depths down to the ocean floor. This need not happen if nonlinearities are permitted a role and if the motion is driven by westward winds; such winds cause divergent flow and hence upwelling. The downward diffusion of momentum can therefore be balanced by the upward advection of water with little zonal momentum. One would therefore expect a nonlinear westward jet to be shallower and less intense than its linear counterpart. Since the poleward advection of momentum in the surface layers is important in a nonlinear model, we also expect a nonlinear westward jet to be broader than a linear one. These inferences are confirmed by the numerical calculations as can be seen in Figs. 4 and 5.

In the case of eastward winds the downward diffusion of momentum is enhanced by the convergent flow in the surface layers, and the associated downwelling. Nonlinear eastward jets should therefore be narrower, deeper and more intense than their linear counterparts. Fig. 5 shows that this is indeed the case. In Fig. 4 we see how the downward diffusion of momentum at the equator is affected by nonlinear advection. Fig. 6 shows the effect of

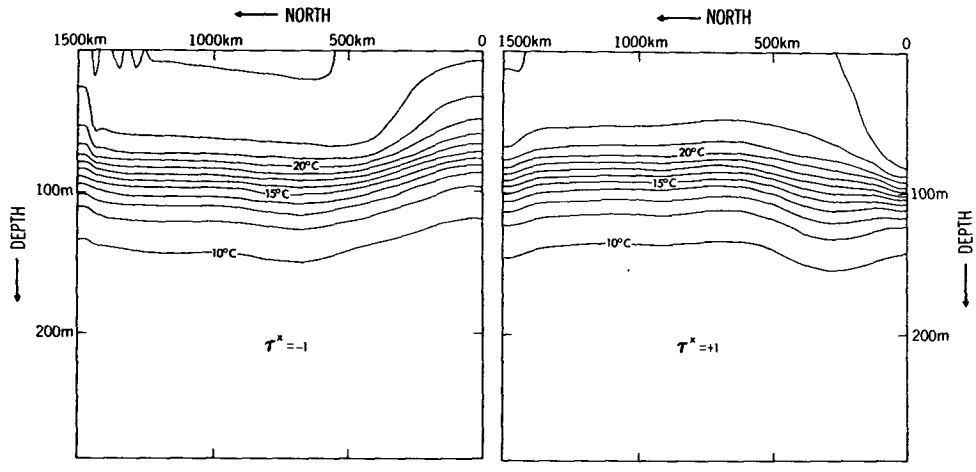

FIG. 6. The temperature field, in a meridional plane, associated with the nonlinear flow patterns in Fig. 5.

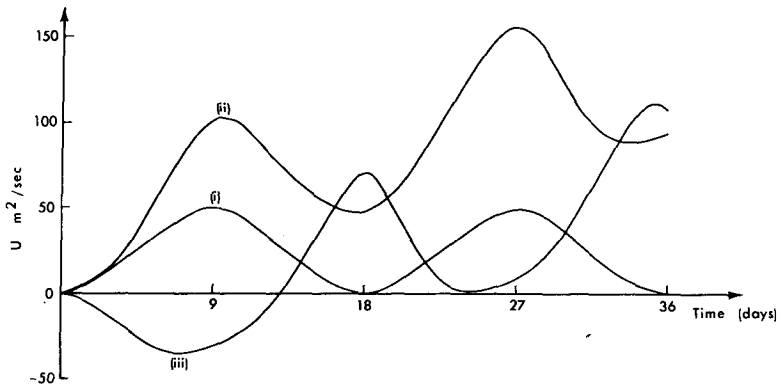

FIG. 7. The vertically integrated zonal transport at the equator in response to the wind-stress given in (5) according to (i) Eq. (6) with $\tau_0 = +1$, (ii) the nonlinear model with $\tau_0 = +1$ and (iii) the nonlinear model with $\tau_0 = -1$.

the convergent and divergent motion on the thermal structure.

Steady-state x-independent flow requires a drag on the ocean floor to balance the imposed surface stress. Before such a state is reached the surface jet will become unstable, and the effects of meridional coasts will become important. (Numerical simulations show that after being forced for a month, the x-independent jet is still accelerating.) Instead of attempting to simulate steady-state conditions, we proceed to study the effect of variable winds.

A linear jet generated by winds that blow in one direction for a certain period of time will be destroyed if the winds reverse direction and blow in the opposite direction for an equal length of time.

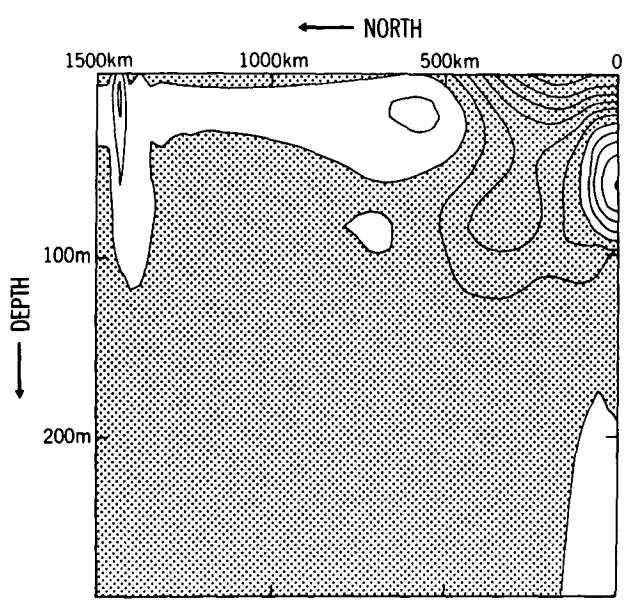

FIG. 8. A meridional section of the zonal velocity component 25.5 days after the onset of the surface winds given by (5) with $\tau_0 = +1$. The shaded flow is westward, contours are at 10 cm s^{-1} intervals.

This will not happen if the flow is nonlinear and if the winds blow in one direction sufficiently long for the jets to be in geostrophic balance. (Geostrophic flow will persist in the absence of any forcing.) This is so because eastward winds generate a jet of greater intensity and greater depth than do westward winds of the same strength. Consider the response to the wind stress

$$\tau^x = \tau_0 \sin(\sigma t),$$

where

$$\sigma = \frac{2\pi}{18 \text{ days}}. \tag{7}$$

Such a wind blows eastward for nine days, then westward for nine days, and has a maximum intensity of 1 dyn if $\tau_0 = 1$. We have chosen nine days for the time scale because it is sufficiently long for nonlinear processes to become important and because it is sufficiently long for a geostrophic zonal equatorial current to become established. According to the linear equation (6) the vertically integrated zonal transport at the equator in response to the oscillatory wind stress (7) is

$$U = \frac{\tau_0}{\sigma}(1 - \cos\sigma t). \tag{8}$$

After a full cycle this transport is zero. Fig. 7 shows that nonlinearities can introduce a hysteresis because of the difference between nonlinear eastward and westward jets. After 25.5 days, at which time the surface winds are blowing westward, the currents have the vertical structure shown in Fig. 8. Fluctuating winds with a time scale longer than a week clearly can produce equatorial currents with a complicated vertical structure.

4. Coastal jets

Near coasts, Ekman layers are well-behaved and do not have singularities, as they do near the equator.

In coastal regions, however, the Ekman suction has a discontinuity right at the coast. For example, a steady wind stress that is parallel to a coast on an f plane drives a nondivergent Ekman layer, with a transport τ^x/f perpendicular to the coast. This transport must vanish at the coast so that a narrow diffusive boundary layer is necessary there. This boundary layer is so narrow compared to the radius of deformation that, on the latter scale, there is effectively a point source (or sink) of fluid at the coast. (In our numerical model the width of this boundary layer is effectively the distance of the first grid point from the coast.) The motion below the Ekman layer can be considered driven by this corner sink. In an ocean initially at rest, the time it takes to establish an Ekman layer is an inertial period. Our numerical calculations show that on longer time scales a coastal jet which was first studied by Charney (1955) is the most prominent feature of the flow. Fig. 9 shows this zonal jet, the associated meridional circulation, and the temperature field 4.5 days after the onset of alongshore winds of intensity 0.5 dyn. If the winds continue to blow, the flow pattern will in due course change when a bottom Ekman layer is formed and a steady state is approached (Allen, 1973). In our

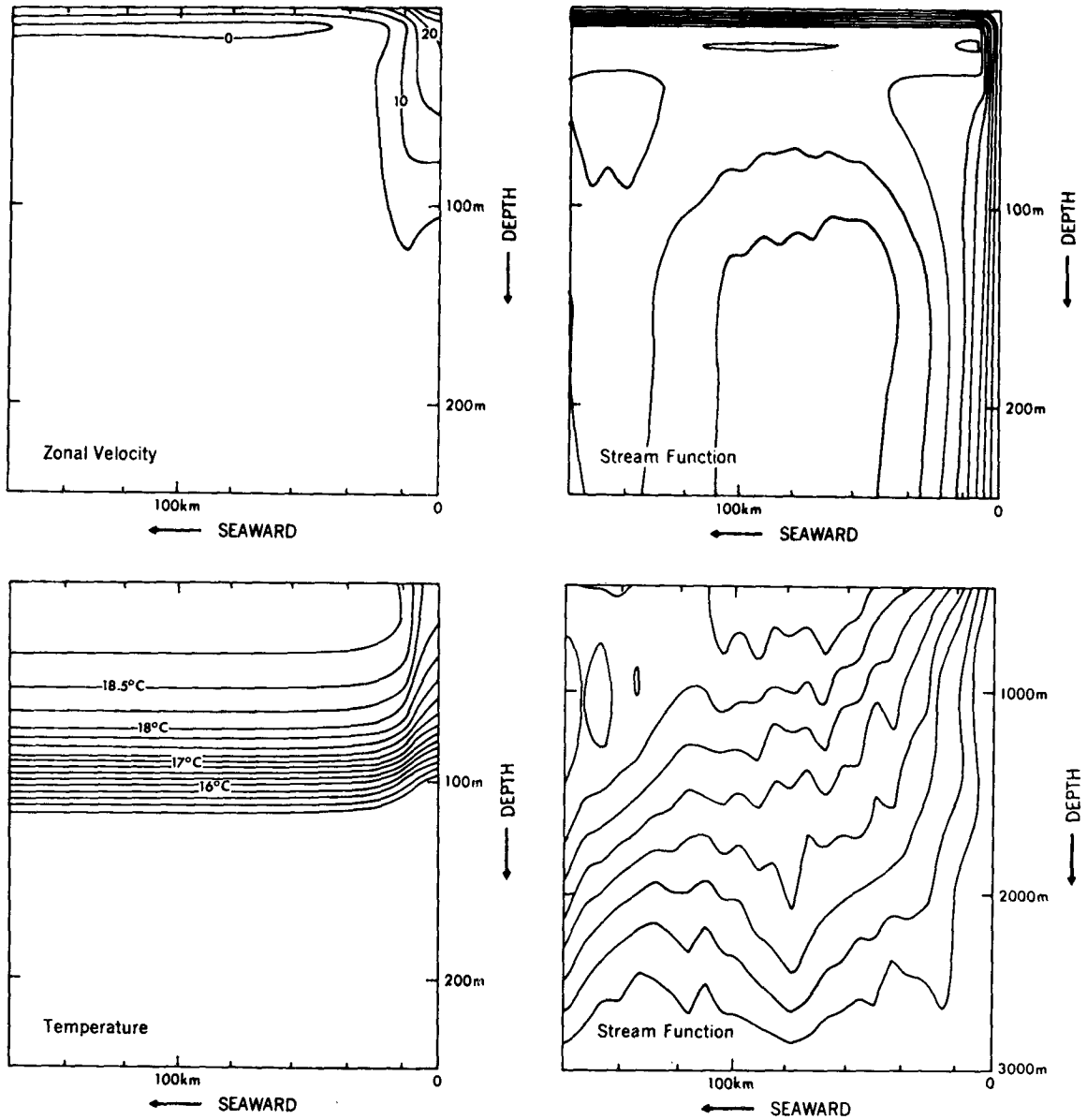

FIG. 9. Structure of a coastal jet 4.5 days after the onset of winds of intensity 0.5 dyn parallel to the coast. Contours for the streamfunction (in the two right-hand panels) are in units of 10^3 m^2 s^{-1}.

model this happens after several weeks. We therefore address the question whether nonlinearities could alter the oceanic response before a steady state is approached. Surprisingly, nonlinear calculations of the responses to wind stresses of intensity 0.5 dyn, that cause upwelling in one case and downwelling in another, do not show substantial departures from the linear solutions. After 10 days, by which time the linear jet attains a maximum speed of 70 cm s^{-1} and the nonlinear jets attain maximum speeds of 62 cm s^{-1}, the flow patterns look the same; at that stage all the jets have essentially the same width and depth. The details of the flow pattern in the corner that acts as sink (or source) will be strongly affected by nonlinearities but for our purposes we are only interested in the role of this corner as a source (or sink).

Pedlosky's (1978a,b) recent study of the nonlinear structure of coastal jets differs from this one in that his model ocean is not initially at rest but is forced by a geostrophic coastward flow. Because the initially imposed motion is in geostrophic balance there exists an alongshore pressure force which, on an f plane, implies the existence of a second coast perpendicular to the first one. Our two-dimensional model cannot be used to simulate flow patterns such as those described by Pedlosky. A further difference is the presence of dissipative processes in this model but not Pedlosky's. A study with a three-dimensional model (which permits alongshore pressure gradients) will be valuable. Meanwhile, we conclude that nonlinearities affect coastal and equatorial jets differently.

5. Discussion

Knox's (1976) weekly profiles near Gan describe the evolution of a wind-driven eastward equatorial jet. His estimates of the magnitudes of the linear terms in the zonal momentum equation indicate an imbalance. Our study shows that the nonlinear terms need to be taken into account within a week after the winds start to blow. A simulation of the Indian Ocean jet, which uses the 3 h winds measured at Gan to drive the model described in Section 2, is reasonably successful for the first 40 days after the onset of the intense eastward winds. Thereafter the jet in the two-dimensional model continues to accelerate but the observed jet does not. It can be shown that the effect of meridional coasts and the zonal pressure gradients they support are important everywhere along the equator within a month (Cane, 1979). A further attempt to simulate the eastward equatorial jet will therefore be made with a three-dimensional model.

The winds at Gan are highly variable and in the early spring are westward for prolonged periods, before intense eastward winds prevail. The same is presumably true of the winds further west. If the winds persist in any one direction for more than a week, a geostrophic jet will be generated. This will give the ocean a "memory" because the jet will continue even when the winds relax. A reversal in the direction of the wind could destroy this jet, but this is unlikely if the flow is nonlinear. As shown in Section 3 and in Fig. 8, the nonlinear response to winds that reverse their direction can have a complicated vertical structure near the equator. In a three-dimensional ocean, the finite zonal extent of the basin will result in the decay of these jets into equatorial (primarily Rossby) waves. The small vertical scales of the jets imply that the waves they radiate will have short vertical wavelengths. Such waves have small group velocities so that the jets will persist for a considerable time.

Luyten and Swallow (1976) observed that the flow near the equator along 55°E in the Indian Ocean had a complicated vertical structure in May and June 1976. The results described here suggest that the alternating jets they observed in the surface layers could have been wind-generated geostrophic currents. It is improbable that this mechanism can account for reversals in the direction of the zonal flow below a depth of a few hundred meters.

The meridional section shown in Fig. 8 is similar to cross-equatorial sections in the Atlantic and Pacific Oceans in that an eastward subsurface jet is imbedded in a westward current. This clearly is not a model of the Equatorial Undercurrent, however, because the Undercurrent observed in the Pacific and Atlantic Oceans is not generated by winds that reverse direction. (An eastward pressure force plays a central role in the momentum balance of the observed Undercurrent.) But there is one respect in which the dynamics of this model is similar to that of the observed Undercurrent. Gill (1975) pointed out that the meridional circulation (with which is associated convergent equatorward flow in the thermocline at the depth of the core of the Undercurrent) is such that the Reynolds stresses provide eastward momentum to the Undercurrent. For this mechanism to be important the flow must be nonlinear. It follows from a scale analysis that the width of the current is $(U/\beta)^{1/2}$, where U is a measure of the speed of the current. This length scale is 220 km (if $U = 1$ m s^{-1}) which is substantially larger than 120 km, the half-width of the observed Undercurrent. A scale analysis yields the same results for eastward and westward jets. Our model shows that nonlinearities make eastward jets narrower than westward jets and therefore could provide an explanation for the narrowness of the Equatorial Undercurrent.

Upwelling in the Gulf of Guinea has recently attracted much attention [see Philander (1979) for a discussion of the various models]. Apparently

local winds cause both equatorial upwelling and coastal upwelling along the nearly east-west coast at about 5°N. The question is whether the two upwelling regions overlap. The radius of deformation for the first baroclinic mode has such a large value in this Gulf that it would appear that even in a simple longitude-independent model, coastal upwelling cannot be isolated from equatorial upwelling. The discussion in Section 3, however, indicates that the radius of deformation associated with the first baroclinic mode is not the appropriate length scale. The correct length scale will be shorter since the vertical scale of the surface phenomena is smaller than that of the first baroclinic mode. Calculations, with the model of Section 2, for the Gulf of Guinea confirm that the scales of the coastal and equatorial upwelling regions are sufficiently small for these upwelling regions not to overlap.

Acknowledgments. It is a pleasure to acknowledge several enlightening conversations with Dr. Moore. Drs. Orlanski and Ross generously made available to me the numerical program that solves the equations described in Section 2. Mr. Tunison and Ms. Kennedy provided expert technical assistance.

REFERENCES

Allen, J. A., 1973: Upwelling and coastal jets in a continuously stratified ocean. *J. Phys. Oceanogr.*, **3**, 245–257.

Arakawa, A., 1966: Computational design for long term numerical integration of the equations of motion: Two-dimensional incompressible flow. *J. Comput. Phys.*, **1**, 119–143.

Cane, M., 1979: The response of an equatorial ocean to simple wind-stress patterns. To appear in *J. Mar. Res.*

Charney, J. G., 1955: The generation of oceanic currents by winds. *J. Mar. Res.*, **14**, 477–498.

Gill, A. E., 1975: Models of equatorial currents. *Proc. Symp. Numer. Models Ocean Circ.*, Durham, Nat. Acad. Sci., 181–203.

Knox, R., 1976: On a long series of measurements of Indian Ocean equatorial currents near Addu Atoll. *Deep-Sea Res.*, **23**, 211–221.

Lilly, D. K., 1965: On the computational stability of numerical solutions of time-dependent, non-linear geophysical fluid dynamics problems. *Mon. Wea. Rev.*, **93**, 11–26.

Luyten, J., and J. Swallow, 1976: Equatorial undercurrents. *Deep-Sea Res.*, **23**, 1005–1007.

Mooers, C. N. K., C. A. Collins and R. L. Smith, 1976: The dynamic structure of the frontal zone in the coastal upwelling region off Oregon. *J. Phys. Oceanogr.*, **6**, 3–21.

Moore, D. W., 1979: Wind-driven motion in a stratified ocean with vertical mixing. Manuscript in preparation.

——, and S. G. H. Philander, 1977: Modeling of the tropical oceanic circulation. *The Sea*, Vol. 6, E. D. Goldberg, Ed., Wiley, Chap. 8, pp. 319–361.

O'Brien, J. J., and H. E. Hurlburt, 1974: Equatorial jet in the Indian Ocean. *Science*, **184**, 1075–1077.

Orlanski, I., and B. Ross, 1973: Numerical simulation of the generation and breaking of internal gravity waves. *J. Geophys. Res.*, **78**, 8808–8826.

Orlanski, I., B. Ross and L. Polinsky, 1974: Diurnal variation of the planetary boundary layer in a mesoscale model. *J. Atmos. Sci.*, **31**, 965–989.

Pedlosky, J., 1978a: An inertial model of steady coastal upwelling. *J. Phys. Oceanogr.*, **8**, 171–177.

——, 1978b: A nonlinear model of the onset of upwelling. *J. Phys. Oceanogr.*, **8**, 178–187.

Philander, S. G. H., 1979: Upwelling in the Gulf of Guinea. *J. Mar. Res.*, **37**, 23–33.

Wyrtki, K., 1973: An equatorial jet in the Indian Ocean. *Science*, **181**, 262–264.

Yoshida, K., 1959: A theory of the Cromwell Current and equatorial upwelling. *J. Oceanogr. Soc. Japan*, **15**, 154–170.